

Chaos in Chemoton Dynamics

Andreea Munteanu
Ricard V. Solé

SFI WORKING PAPER: 2005-05-017

SFI Working Papers contain accounts of scientific work of the author(s) and do not necessarily represent the views of the Santa Fe Institute. We accept papers intended for publication in peer-reviewed journals or proceedings volumes, but not papers that have already appeared in print. Except for papers by our external faculty, papers must be based on work done at SFI, inspired by an invited visit to or collaboration at SFI, or funded by an SFI grant.

©NOTICE: This working paper is included by permission of the contributing author(s) as a means to ensure timely distribution of the scholarly and technical work on a non-commercial basis. Copyright and all rights therein are maintained by the author(s). It is understood that all persons copying this information will adhere to the terms and constraints invoked by each author's copyright. These works may be reposted only with the explicit permission of the copyright holder.

www.santafe.edu



SANTA FE INSTITUTE

Chaos in chemoton dynamics

Andreea Munteanu^{1,*} and Ricard V. Solé^{1,2}

¹ ICREA-Complex Systems Lab, Universitat Pompeu Fabra (GRIB), Dr Aiguader 80, 08003 Barcelona, Spain
² Santa Fe Institute, 1399 Hyde Park Road, Santa Fe NM 87501, USA

Gánti's chemoton model (Cell.Biol.Int. 26, 729, 2002) is considered as an iconic example of a minimal protocell including three key ingredients: membrane, metabolism and information. The three subsystems are coupled and it is suggested they guarantee a stable, homeostatic replication cycle. However, a detailed exploration of the model indicates that it displays a wide range of complex dynamics, from regularity to chaos. Here we report the presence of a very rich set of dynamical patterns potentially displayed by a protocell as described by the chemoton model. The implications for early cellular evolution and synthesis of artificial cells are discussed.

Keywords: Protocell, origins of life, chemoton, cellular networks, chaos

I. INTRODUCTION

Cells are the basic building blocks of all life on our planet. They are the minimal systems able to self-replicate in a regular manner and evolve through changes in genetic information. Understanding how cellular life emerged is one of the most challenging problems in life sciences. The early origin of cellular life was certainly not associated to a complex membrane with a long genome and intricated metabolic pathways. Instead, it is believed to have been the result of coupled, simple chemical reactions that allowed evolution to act on replicating nanostructures. Theoretically, this hypothesis is the basis of the most relevant modelling approaches available in the literature [8]. Experimentally, the moment of the synthesis of an artificial nanocell based on this theory seems to be closer than ever [7].

What are the minimal building blocks of a self-replicating protocell? This is a fundamental question of both theoretical and practical relevance. At its fundamental level, it becomes linked with early conjectures about what is required in order to have self-replication. Pioneering work by von Neumann revealed that a machine able to replicate itself needed three basic ingredients which can be easily identified with the key components found in real cells in our current biosphere (see [4] and references therein). More precisely, all cells deal with the three basic components of cellular networks: metabolism, information and membrane [1]. All cells replicate their hereditary information through template polymerization, which is stored in the same linear chemical code (the DNA). In order to sustain life, cells have to be in a nonequilibrium state, taking free energy from the environment. Raw materials are used to drive the chemical reactions inside the cell body with the help of proteins acting as catalysts. The result of cellular evolution is a complex set of structures that allow living forms to survive and exchange information with the environment. Beyond the specific paths used, they all share a common trait: they operate in closed cycles and define a non-separable whole.

Simple, minimal protocells should be able to sustain a reliable replication cycle, properly coupling the components in

a way that they help each other. Clearly, once a threshold of chemical complexity is reached, nonlinear phenomena are likely to develop. In this context, it is relevant to ask what types of dynamical patterns are expected to occur when an arbitrary set of conditions are used to build a protocell: are stable replication cycles a generic feature of a coupled set of cellular components? Can nonlinearities jeopardize the presence of a stable cell cycle and potential heredity? Is the complexity of templates a key ingredient in sustaining reliable replication? Little is known about these questions. In this paper we want to address them by means of a numeric study of the so called *chemoton* model. This model is a simple, but rich approach to protocellular dynamics. It has been used as a prototype model of cellular life. As shown here, very complex dynamical patterns can be observed even at this simple level, thus suggesting that the richness of potential dynamical behaviors exhibited by protocells can be high. Besides, it generates new evolutionary questions to be answered by future experiments in this area.

II. CHEMOTON MODEL

As the driving force of living systems is the chemical energy and as chemical reactions can proceed with suitable intensity only in fluid phase, generally a solution, living systems can be thought to have as a fundamental unit a fluid automata

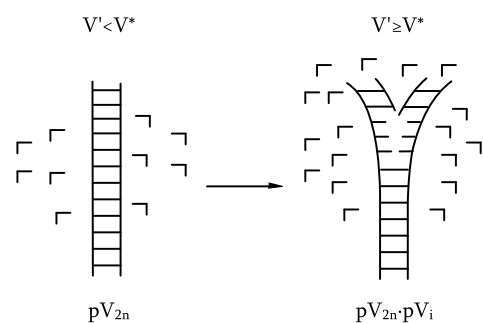


FIG. 1: Template chains may open randomly and for monomers' concentration V' below the critical threshold V^* , the opposite ends reconnect. For $V' \geq V^*$, bonding with available monomers can occur, leading to the zip-like replication of the polymer pV_{2n} .

*Corresponding author: E-mail: andreea.munteanu@upf.edu; Phone: +34 935422834; Fax: +34 932213237

TABLE I: Chemical reactions of the chemoton model

Metabolism	Membrane	Template
$A_1 + \bar{X} \xrightleftharpoons[k_1']{k_1} A_2$		
$A_2 \xrightleftharpoons[k_2']{k_2} A_2 + \bar{Y}$		replication initiation: $pV_{2n} + V' \xrightleftharpoons[k_6']{k_6} pV_{2n} \cdot pV_1 + R$
$A_3 \xrightleftharpoons[k_3']{k_3} A_4 + V'$	$T' \xrightarrow{k_8} T^*$	replication propagation: $pV_{2n} \cdot pV_i + V' \xrightarrow{k_7} pV_{2n} \cdot pV_{i+1} + R,$
$A_4 \xrightleftharpoons[k_4']{k_4} A_5 + T'$	$T^* + R \xrightleftharpoons[k_9']{k_9} T$	$1 \leq i \leq 2n - 1$
$A_5 \xrightleftharpoons[k_5']{k_5} A_1 + A_1$		$pV_{2n} \cdot pV_{2n} \rightarrow pV_{2n} + pV_{2n}$

endowed with the following properties: to function under the direction of a program, to be separated from the environment and to reproduce itself. Gánti first described such a model in 1971, where the program-controlled self-reproducing fluid automata was called chemoton – see review [6].

The chemoton consists in three functionally dependent autocatalytic subsystems: the metabolic chemical network, the template polymerization and the membrane subsystem enclosing them all. The self-reproducing metabolic network transforms the external nutrients into chemoton's internal material necessary for template replication and membrane growth.

The second subunit consists in the self-replication of a double-stranded template. For the double-stranded templates, the chain ends can open due to inherent fluctuations, but with high probability the corresponding monomers of the opposite strands reconnect. If a sufficiently high concentration of monomers is present, the bonding can also take place with free monomers, leading to a zipper-like opening of the double-stranded complex and to its replication (Fig 1). Once the initiation step has occurred, the secondary bonds are more probable to open up, and thus the addition of new monomers is supposed to propagate quite fast. It is an oversimplified version of the semiconservative DNA replication where the two strands of the parental double helix unwind and each specifies a new daughter double-strand by base-pairing rules.

The program-controlled role of the template replication consists in the fact that the monomers would not polymerize until they have reached a certain concentration. The control thus implies the regulation of the monomer consumption in the copying process, depending on the number of template molecules present and the length of the strands, i.e. the number of monomers needed to synthesize a new double-strand. As the templates are double, the amount of monomers should also double in order to ensure a stable functioning of the automata, leading to the necessity of the autocatalytic nature of the metabolic subunit.

The third subunit is a model of a two-dimensional membrane forming a spherical enclosure of the system. Once the amount of monomers passes the required threshold value, the template replication starts and its waste products react with the membrane precursors producing real membrane molecules which are spontaneously incorporated in the membrane, thus increasing its surface and implicitly the chemoton's volume.

Once again it discloses the controlling and coordinating role of the template subunit.

The correct functioning of the chemoton lies in the precise stoichiometric coupling of the three subunits, more precisely the coordination between the accumulation of molecules and the surface increase in order to achieve an equilibrium of the osmotic pressure relative to the environment. If the concentration of molecules increases rapidly, the microsphere bursts when the osmotic pressure reaches a critical value. On the other hand, if the increase of the autocatalytic and membrane molecules is parallel and exponential, with a similar growth of the microsphere surface, the liquid becomes diluted and the sphere decompresses. Gánti (2002) argues that in order to resolve the instability by division into two identical spheres in osmotic equilibrium with their environment, the chemoton

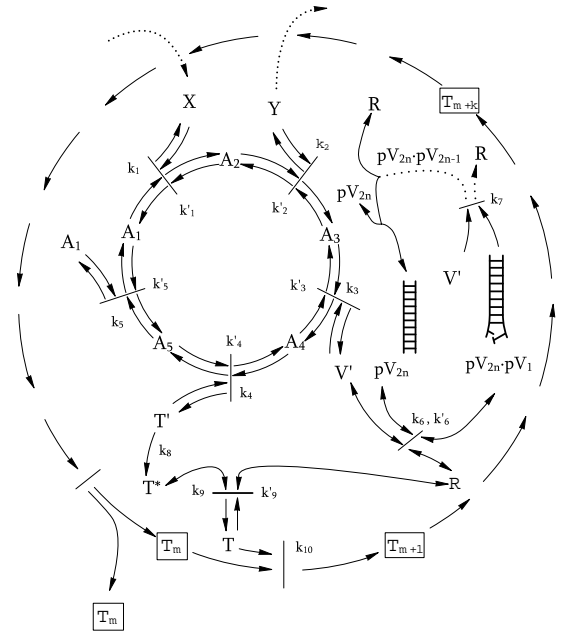


FIG. 2: The chemoton: the metabolic unit, the template (information) subunit and the membrane subsystem. The dots in the template subsystem indicate the iterative development of the template replication from $pV_{2n} \cdot pV_1$ to $pV_{2n} \cdot pV_{2n-1}$.

must reach a state where both the surface and the inner components have doubled their initial amount [5]. At this precise moment, it is assumed that, due to the concentration decay, an osmotic vacuum develops and the membrane sphere is elongated, with a neck forming in the middle leading to the subsequent division (none of these physical events are really introduced in the model explicitly).

As defined, the model would allow a cycle stoichiometric coupling of the autocatalytic cycles such that the number of membrane molecules necessary for surface doubling is equal to the number of polymerization iterations needed for complete replication of all template molecules. For example, (Gánti 2003) let us assume a sphere of 10 million molecules membrane and 10^5 simple strand templates. In order for the chemoton to double its surface and template molecules, the strands must be composed of 10^2 nucleotides [6].

One can notice that the total number of templates somehow “genetically” influences the size of the chemoton (a simple phenotypic trait) as well as its replication time. As a consequence of this interdependence, the statistical halving of the number of template molecules leading to possible differences in the number of templates in the offspring cells might introduce hereditary changes and genetic diversity of chemoton populations [6].

III. THE MODEL

Unfortunately, the chemoton model introduced and studied by Gánti in several papers has drawn the attention of only a few scientists: Csentes (1984) and Fernando& Di Paolo (2004) - [2, 3]. Within the general approach to chemical reaction networks, simulations of the chemoton model used the standard kinetic differential equations providing the temporal evolution of the metabolites’ concentrations. More realistic simulations are presented in [3] where a discrete probabilistic treatment of the template replication is coupled with a continuous deterministic treatment of the metabolism and membrane subunits. However, no complete stochastic simulation of the chemoton model has been performed so far.

Table I includes the chemical reactions of the chemoton model, where k_i are the rate constants. The members of the metabolic autocatalytic cycle are denoted as A_1, \dots, A_5 . The five elements are produced from A_1 through a closed cycle involving five reactions: the consumption of the external nutrient X , the formation of waste Y , of template and membrane precursors, V' and T' , respectively, and the closing step of the autocatalytic cycle producing two A_1 (see Table 1). It is assumed that a large quantity of nutrient X is available and that the waste Y is eliminated through the membrane in such manner that the number of X and Y molecules can be considered as constant, denoted as \bar{X} and \bar{Y} . One can notice that at least one of the metabolism molecules must be present at an initial moment inside the chemoton in order to ensure the metabolism functioning and thus chemoton’s survival. In accordance with these chemical reactions, the kinetic differential equations describing the temporal evolution of the chemical system are included in Table II, where the upper dot im-

TABLE II: Kinetic differential equations of the chemoton model

\dot{A}_1	$= 2(k_5 A_5 - k'_5 A_1 A_1) - k_1 A_1 \bar{X} + k'_1 A_2$
\dot{A}_2	$= k_1 A_1 \bar{X} - k'_1 A_2 - k_2 A_2 + k'_2 A_3 \bar{Y}$
\dot{A}_3	$= k_2 A_2 - k'_2 A_3 \bar{Y} - k_3 A_3 + k'_3 A_4 V'$
\dot{A}_4	$= k_3 A_3 - k'_3 A_4 V' - k_4 A_4 + k'_4 A_5 T'$
\dot{A}_5	$= k_4 A_4 - k'_4 A_5 T' - k_5 A_5 + k'_5 A_1 A_1$
\dot{V}'	$= k_3 A_3 - k'_3 A_4 V' + k'_6 pV_{2n} \cdot pV_1 R -$ $- k_6 pV_{2n} V' - \sum_{i=1}^{2n-1} k_7 pV_{2n} \cdot pV_i V'$
\dot{R}	$= k_6 pV_{2n} V' - k'_6 pV_{2n} \cdot pV_1 R + k'_9 T -$ $- k_9 T^* R + \sum_{i=1}^{2n-1} k_7 pV_{2n} \cdot pV_i V'$
\dot{T}'	$= k_4 A_4 - k'_4 A_5 T' - k_8 T'$
\dot{T}^*	$= k_8 T' - k_9 T^* R + k'_9 T$
\dot{T}	$= k_9 T^* R - k'_9 T - k_{10} T S$
\dot{S}	$= k_{10} T S$
$p\dot{V}_{2n}$	$= 2k_7 pV_{2n} \cdot pV_{2n-1} V' + k'_6 pV_{2n} \cdot pV_1 R -$ $- k_6 pV_{2n} V'$
$\underbrace{pV_{2n} \cdot pV_1}$	$= k_6 pV_{2n} V' - k'_6 pV_{2n} \cdot pV_1 R -$ $- k_7 pV_{2n} \cdot pV_1 V'$
$\underbrace{pV_{2n} \cdot pV_{i+1}}$	$= k_7 pV_{2n} \cdot pV_i V' - k_7 pV_{2n} \cdot pV_{i+1} V'$ $1 < i < 2n - 1$

plies a derivative with respect to time.

As a particularity, the k_8 -equation was considered as necessary by Csentes (1984) “since otherwise in the case of certain k_i and k'_i the accumulated T' might make the autocatalytic cycle slow down still before R , originated from the pV_{2n} synthesis, might extract it.”

The membrane subsystem obtains the precursor molecules from the other two subunits and transforms them into a proper membrane molecule T (second column of Table I). *These molecules are spontaneously incorporated into the membrane’s molecules and the speed of the process is proportional to the membrane surface area S , with a proportionality coefficient k_{10} (Csentes 1984).*

We denoted the double-stranded template molecules as pV_{2n} indicating its composition, formed by two simple strands of n pieces of monomer V' . As in the previous studies, we consider the template replication in a zipper-like form as expressed above, where a waste molecule R is also produced (see the third column of Table I). Overall, the template replication ensures that exactly as many V' are necessary to replicate the pV_{2n} templates as many T are produced and are needed to equal the double of the initial number of membrane molecules.

The reaction rate constant of the initiation for the template replication is $k_6 = 0$ for $V' < V^*$, where V^* is the monomer threshold associated to replication initiation. The template replication initiates once the condition $V' \geq V^*$ is fulfilled. At this moment, k_6 acquires a nonzero value and the surface, and implicitly the volume, of the chemoton starts to

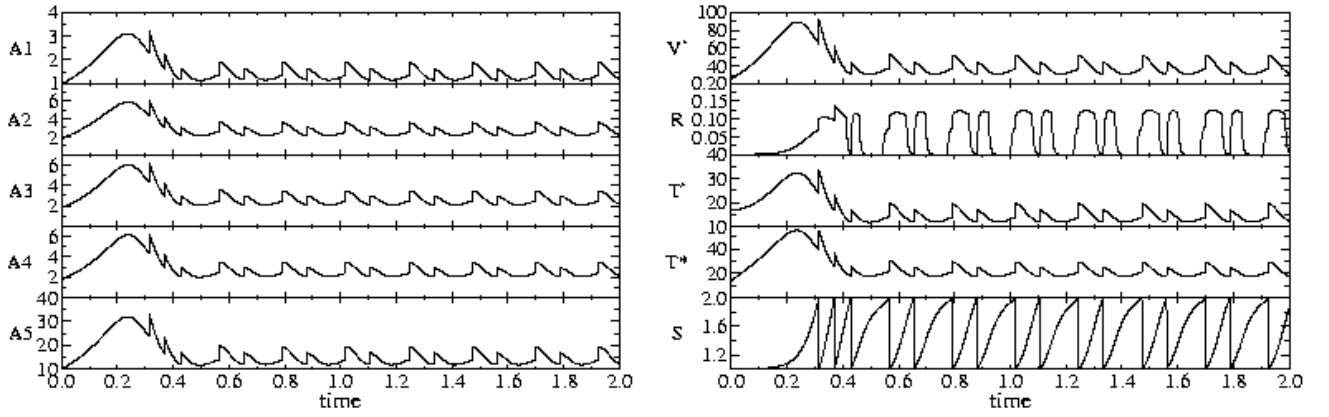


FIG. 3: Time series of metabolites concentration for the strong condition of template replication: $\bar{X} = 100$, $N = 25$, $V^* = 35$. This case presents two self-replication periods. One can notice that the concentrations increase after division. The surface is denoted by S .

grow. When the surface doubles its initial value, the chemoton is assumed to divide, a process interpreted as the halving of its surface and all its metabolites, and the system of differential equations resumes integration with the new values of the metabolites' concentrations.

The volume is not explicitly introduced in the model and therefore neither in the equations system describing the temporal evolution of the concentrations. However, the concentrations depend intrinsically on the volume. Thus, in order to obtain their correct value at each step, one must rescale them to the new volume resulting from the increase of surface S . This implies that, once the template replication and also surface growth start, after each step i , one must multiply the resultant concentrations by the factor

$$f = \frac{V_{i-1}}{V_i} = \left(\frac{S_{i-1}}{S_i} \right)^{3/2}, \quad (1)$$

with the resulting values being used as input conditions for the

next integration step. Since concentrations are given in moles per volume, the division, as defined here, implies the halving of both moles and surface. This entails the multiplication of the concentrations at division with a factor $div = 0.5 * f = \sqrt{2}$, with $f = 2^{3/2}$. It is a consequence, on one hand, of the halving in moles and, on the other hand, of the volume rescaling factor as $S_b = 2S_a$, with b and a referring to the values before and after division, respectively. One can notice that the concentrations of the substrates increase at splitting.

This rescaling is not performed in [2], while in [3] it is discussed, but not included in the simulation, as one can see in their Fig. 2 that the concentrations decrease at division. This introduces a warning with respect to the results they obtain and their interpretation. Their main results concern the dependence of the chemoton's replication time on the main parameters of the model, such as monomers threshold V^* , template length N or nutrient concentration \bar{X} . Interesting enough, Csentesi (1984) obtains that longer templates have lower replication times at low levels of nutrient concentration, implying

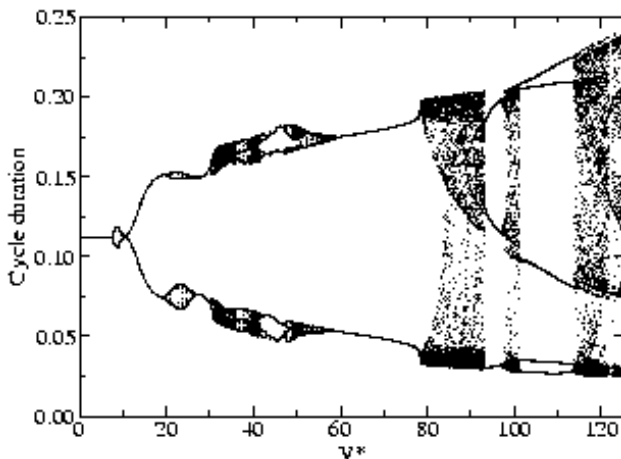


FIG. 4: Dependence of the replication time on the monomers threshold for the case of strong replication condition with $N = 10$ and $\bar{X} = 100$.

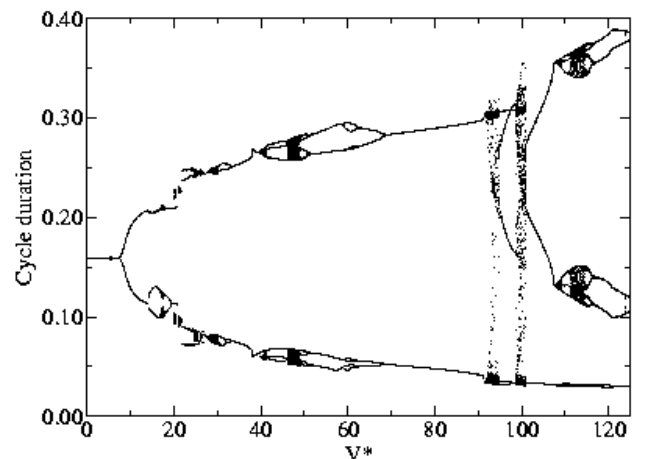


FIG. 5: Dependence of the replication time on the monomers threshold for the case of strong replication condition with $N = 10$ and $\bar{X} = 10$.

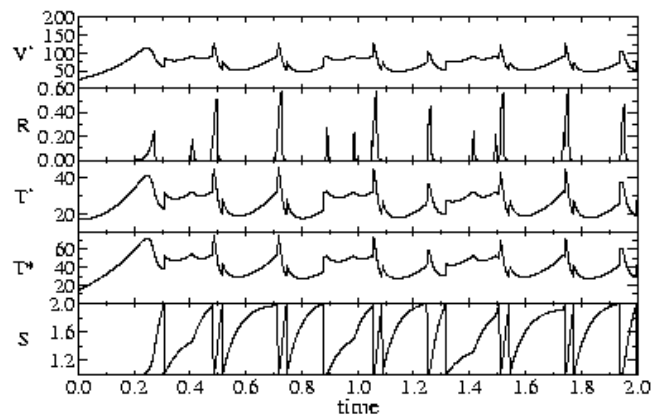
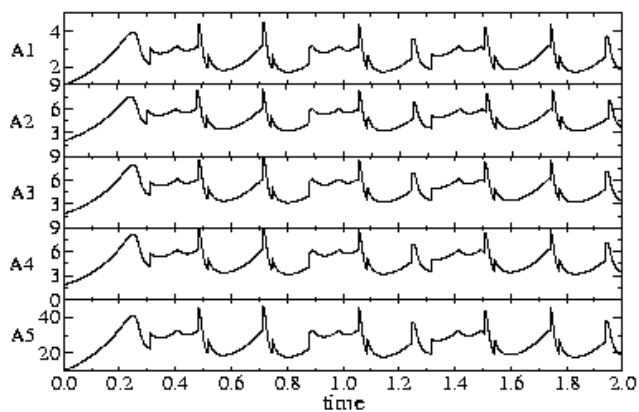


FIG. 6: Time series of metabolites concentration for the strong condition of template replication: $\bar{X} = 100$, $N = 10$, $V^* = 90$. This case is representative for a dynamics characterized by a diversity of self-replication periods. See Fig. 4.

an increased fitness in harsher environments. Fernando & Di Paolo (2004) disprove this result, but discuss the kinetic conditions that could lead longer-templates chemoton into faster replication [3].

IV. RESULTS

As mentioned above, none of the previous works on chemoton dynamics include explicitly the rescaling of the variables due to volume increase. Such a correction is of high importance in order to obtain an appropriate mapping between the implicit cell division occurring in this model and what is likely to occur in real protocells. Using the previous set of equations and the rescaling of concentrations, we can now analyze the expected dynamical patterns and transitions to be observed in a protocell.

A. Strong replication condition

A strong condition for the template replication can be considered as the case in which the replication - initiation and propagation - occurs only for values of monomer concentration above the threshold value. We present the time series associated to this dynamics in Fig. 3. One can notice the existence of multiple self-replication periods. Moreover, a detailed analysis of the dependence of the replication time on the monomer concentration shows a highly nonlinear behavior, as illustrated in Fig 4 for the case of $N = 10$ and $\bar{X} = 100$. Here a bifurcation diagram has been constructed. It shows intervals of the threshold value for which the cycle duration is the same, while for other intervals it is chaotic.

In particular, a bifurcation occurs at $V_c^* \approx 9$ leading to two different, alternating protocell cycle lengths. As V^* grows further, successive bifurcations (including period doubling and halving) take place and the range of cycle durations widens. This observation indicates that, in the chaotic domain, a homogeneous initial cell population with similar initial conditions would change towards a system with an heterogeneous spectrum of cell sizes. Additionally, the requirement that $V \geq V^*$ implies that conditions for template repli-

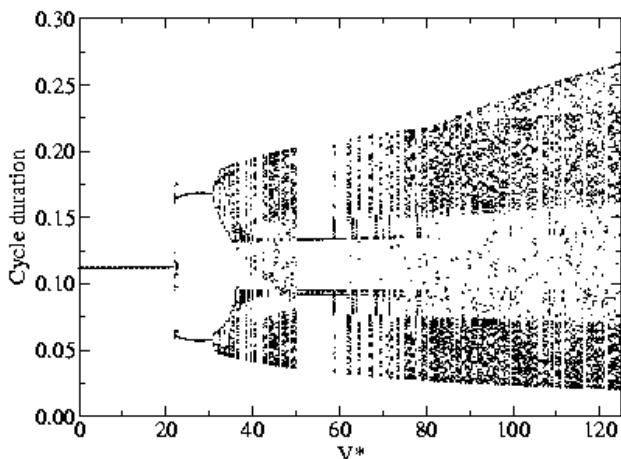


FIG. 7: Dependence of the replication time on the monomers threshold for the case of weak replication condition with $N = 10$ and $\bar{X} = 100$.

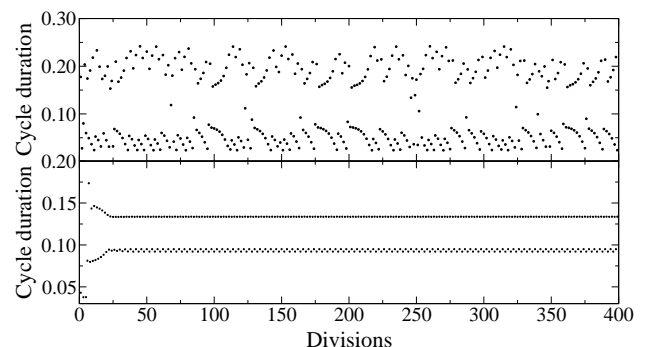


FIG. 8: Temporal evolution of the replication period for $N = 10$, $X = 100$: (upper panel) $V^* = 100$ and (lower panel) $V^* = 55$. See Fig. 7.

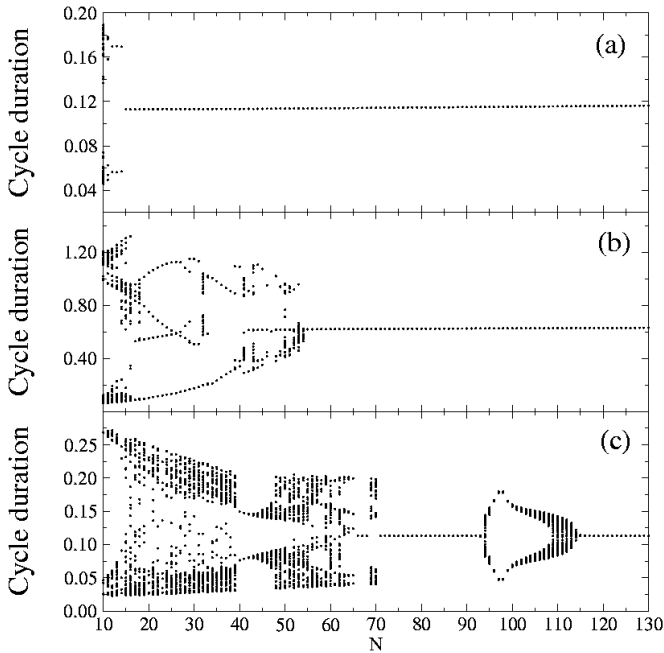


FIG. 9: Dependence of the replication time on the template length for the weak replication condition for the cases of (a) $X = 100$, $V^* = 35$ and $k_7 = 10$; (b) $X = 1$, $V^* = 35$ and $k_7 = 10$; (c) $X = 100$, $V^* = 35$ and $k_7 = 100$.

cation involving high thresholds would be associated to non-stationary replication cycles. This result suggests that, under the present model constraints, evolution would have tuned the efficiency of the polymerization event in order to avoid instabilities.

One can see that a similar dependence of the replication time on the monomer's threshold V^* holds for the case of lower \bar{X} , as can be observed in Fig. 5. As expected, the replication periods are longer since the nutrients are scarce. A more typical illustration of the temporal evolution of the concentrations and as an example of high diversity of replication periods, we include in Fig 6 the time series of the concentrations associated to the case $V^* = 90$ of Fig 4.

Independent of these results, the condition on the template replication discussed above and used for this study appears as too strict to be considered a realistic replication of a double-stranded structure as represented in Fig. 1. More precisely, the theory also suggests that the initiation step acts as a switch to the template replication, with the latter being independent on the monomer concentrations once the initiation has occurred.

B. Weak replication condition

As discussed in the previous section, a more relaxed and realistic condition for the template replication consists in the following approach: the replication can initiate after the monomers reach the threshold concentration, with the propagation of the replication evolving unhindered by the monomers concentration once the initiation has occurred. Our

study still revealed the irregular dependence of the chemoton replication period on the template threshold, as can be seen in Fig. 7. Additional to the bifurcations similar to the previous section, we also show in Fig. 8 an example the temporal evolution of the replication time for a stable and an irregular case of replication.

Fernando&Di Paolo (2004) obtained an optimum value for the template length showing longer replication time, respectively, for either higher or lower template length compared to that optimum value. However, we have to remark from their Fig. 5(b) that the difference in the shortest and longest replication time is of the order of the integration time step, extremely diminishing the significance of an “optimum” value. In Fig. 9, we present our results using the same parameters which lead Fernando&Di Paolo (2004) to their results. One can notice that we obtain a similar dynamics as the one from the previous sections, implying an intrinsic characteristic of the chemoton. Moreover, the differences between our results and the ones existent in the literature suggest that they are a consequence of the way the chemoton responds to the increase of volume. Thus, no optimum value of the template length is apparent from our results. From Fig. 9a,b one can notice that the scarcity of nutrients (low values of \bar{X}) has a significant impact on the dynamics, leading to a more irregular replication at low template lengths.

An even stronger effect in this direction is obtained by increasing the reaction rate of the template replication reaction (k_7) (Fig. 9c) – as performed in Fernando&Di Paolo (2004) – and based on a more realistic approach in which the bottleneck step for the replication is the initiation, with the propagation occurring on a much shorter time scale.

It is interesting to note that template length can be a source of stability. As indicated in figure 7, increasing template length (and this “genome” complexity) leads to a reduction of the variance in cycle periodicity. By suppressing chaos (or at least diminishing its influence) an increase in the complexity of template molecules might be able to stabilize cell replication cycles. Our results thus suggest one possible source of selection towards a more complex cell where, in spite of the higher building cost, larger information carriers might be favored.

V. DISCUSSION

As discussed in the introduction, the chemoton model [5] is an important step toward an integrated model of a protocell capable of performing the essential functions of a living system [7, 9]. The importance of this model relies on the fact that it is the simplest existent model which includes the three essential processing units: the metabolism, the membrane compartment and the “genetic information”. The particularity of the model resides in the stoichiometrical coupling of the three autocatalytic subunits. This coupling ensures the “survival” of the chemoton through the stability of the replication cycle.

Contrary to the existent studies of the chemoton model through the deterministic reaction rate equations, our study of the parameters space of the model reveals parameters ranges

yielding not only stable replication cycle, but also parameter ranges for which various replication periods exist. We recall that the difference between our study and the ones existent in the literature resides in the rescaling of the chemoton's concentrations at each step due to the increase in volume, if it occurs.

The richness of dynamical patterns shown here confirms the commonality of nonlinear behavior found in most biological systems. The presence of reliable, stable cell replication is separated by sharp bifurcations from those less predictable ones. Relevant parameters include continuous ones (such as V^*) and discrete ones (such as template length). The presence of these domains might have nontrivial implications. Just looking at the two parameters explored here, selection towards predictable cell cycles seems to be possible provided that initiation of template replication is efficient enough: low thresholds V^* would be searched for. On the other hand, increasing template complexity might have more benefits than costs: if selection towards fast-replicating cells is at work, it might also require a reduction of fluctuations, which can be achieved by using larger information carriers.

The existence of the irregular replication cycles is relevant especially considering its absence in the previous studies and considering that the volume rescaling is mandatory. At the

first glance, this behavior may be considered as a drawback to the model and an undesired result as it might suggest an intrinsic instability of the replication cycle. On the other hand, it may imply an evolutionary advantage in the perspective of a population of chemotons. More precisely, in the advent of simulating a population of chemotons in order to identify selection effects and population dynamics, the diversity of replication cycles, and implicitly of chemoton "genotypes" may prove to be an advantage. This uncertainty can be resolved only by the simulation itself, and we consider this issue as our future investigation on the chemoton dynamics.

VI. ACKNOWLEDGMENTS

The authors thank Harold Fellermann, Javier Macia, Josep Sardanyes and Sergi Valverde for useful Venetian discussions around protocells and life. We also thank Steen Rasmussen, John McCaskill, Norman Packard and Mark Bedau for useful comments. This work has been supported by EU PACE grant within the 6th Framework Program under contract FP6-002035 (Programmable Artificial Cell Evolution), by MCyT grant FIS2004-05422 and by the Santa Fe Institute.

-
- [1] Alberts, B., Johnson, A., Lewis, J., Raff, M., Roberts, K., Walter, P., 2002. *Molecular Biology of the Cell*. Garland, New York.
 - [2] Csentesi, T., 1984. A simulation study on the chemoton. *Kybernetes* 13, 79.
 - [3] Fernando, C., Di Paolo, E., 2004. The chemoton: A model for the origin of long rna templates. In: Pollack, J., Bedau, M., Husbands, P., Ikegami, T., Watson, R. (Eds.), *Artificial Life IX: Proceedings of the Ninth International Conference on the Simulation and Synthesis of Life*. MIT Press, Cambridge, Massachusetts, pp. 1–8.
 - [4] Freitas, R. A., Merkle, R. C., 2004. *Kinematic Self-replicating Machines*. Landes Bioscience.
 - [5] Gánti, T., 2002. On the early evolution of biological periodicity. *Cell. Biol. Int.* 26, 729.
 - [6] Gánti, T., 2003. *The principles of life*. Oxford University Press.
 - [7] Rasmussen, S., Chen, L., Deamer, D., Krakauer, D. C., Packard, N. H., Stadler, P. F., Bedau, M. A., 2004. Transition from Non-living to Living Matter. *Science* 303, 963.
 - [8] Segré, D., Lancet, D., 2004. Theoretical and computational approaches to the study of the origins of life. In: Seckbach, J. (Ed.), *Origins : Genesis, Evolution and Diversity of Life*. Vol. 6 of COLE. Kluwer Academic Publishers, New York.
 - [9] Szostak, J. W., Bartel, D. P., Luisi, P. L., 2001. Synthesizing life. *Nature* 409, 387.